

Relationships Between Microstructure, Roughness Parameters and Ultrasonic Cavitation Erosion Behaviour of Nodular Cast Iron, EN-GJS-400-15

ION MITELEA, TRAIAN BENA, ILARE BORDEASU*, CORNELIU MARIUS CRACIUNESCU

University Politehnica Timisoara, 2 Victoriei Sq., 300006, Timisoara, Romania

The main objective of this paper is to investigate the influence of microstructure on the degradation of nodular casting by cavitation erosion and the correlation of the surface wear parameters with the sizes that characterize the resistance opposite to the cavitation phenomenon. The cavitation tests were conducted on a vibrator with piezoceramic crystals, respecting the ASTM G32-2010 standard. Microstructural investigations on eroded surfaces were performed on the optical microscope and the scanning electron microscope, and the roughness measurements with the Mitutoyo apparatus. The obtained results have demonstrated the existence of a good correlation between the resistance to cavitation erosion and the roughness parameters R_a , R_z and R_t .

Keywords: nodular cast iron, cavitation erosion, surface roughness

The main reason for triggering the cavitation phenomenon is the drop in pressure in a fluid that flows at high speed. Liquid dissolved in gas is the source of cavitation nuclei. Dynamic loading occurring at the time of cavitation bubble crash takes a period of microseconds or nanoseconds [1-4]. More and more stringent prescriptions for the reliability and durability of process equipment and hydroelectric power generators require a minimization of material degradation through cavitation erosion when working with cavitant and corrosive fluids [5-11].

The incidence of cavitation phenomena can adversely affect such equipment long before damage to the components. Therefore, designers are making extra efforts to design equipment so as to avoid cavitation in the expected range of operation. However, for economic reasons, in the case of complex engineering systems, during normal operation, it is not always possible to completely avoid cavitation. Operation with limited cavitation, without visually affecting component performance parameters, can cause long-term damage. Systematic studies on damage caused by cavitation are required to generate practical value data [12-14]. Research efforts in this field aim at improving erosion resistance by applying volumetric and surface thermal treatments, coatings with protective layers, etc. [10, 11], and on the other hand, prediction of resistance to degradation based on properties mechanical and surface properties of the material [15, 6]. This paper analyzes the possibility of correlating the sizes that characterize cavitation erosion resistance with the hardness and roughness of the surface during the stabilization period of the removal rate of the material.

Experimental part

Material and methods

Cast iron EN-GJS-400-15, with chemical composition: C = 3.57%, Si = 2.51%, Mn = 0.23%, P = 0.044%, S = 0.010% and Fe = rest, were subjected to the heat treatment cycles shown in figure 1.

From the bars thus treated, samples were taken for cavitation tests, microstructural studies, hardness tests and

roughness measurements of the eroded surface. Cavitation tests were run on sets of three samples using a piezoceramic vibrator made in accordance with the requirements of ASTM G32-2010 [17, 18].

Cavitation medium used drinking water from the public network. During the research, the water temperature was maintained at $22 \pm 1^\circ\text{C}$. Before the cavitation test, the attack surface of each sample was polished to a roughness

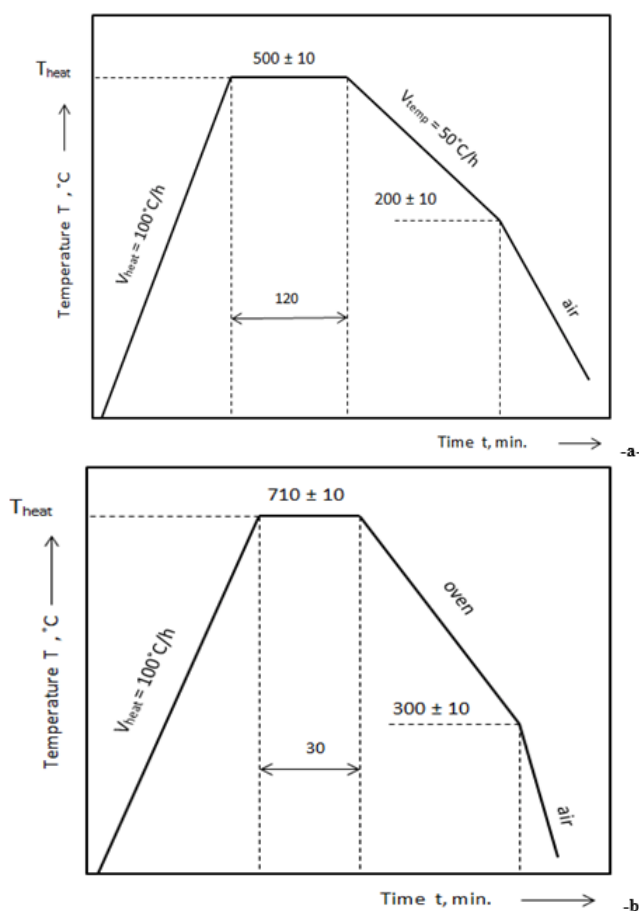


Fig. 1 Cycles of applied heat treatments: a - stress relief annealing; b - softening annealing;

* email: ilarica59@gmail.com; ilare.bordeasu@upt.ro

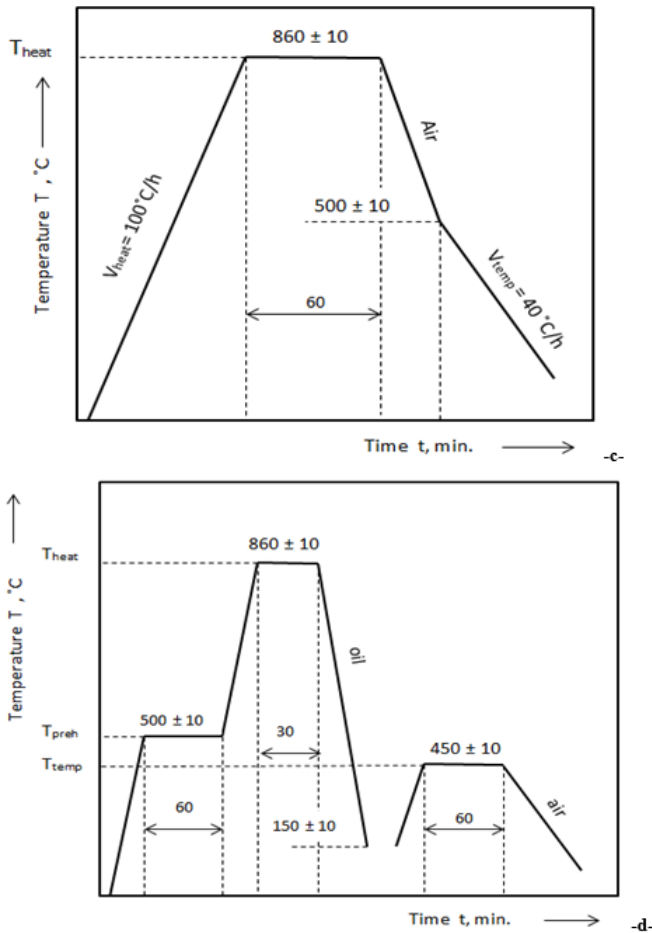


Fig. 1 Cycles of applied heat treatments: c- normalizing; d - quenching + tempering

of $R_a = 0.051 \div 0.090 \mu\text{m}$. During periods of cavitation testing, and until resuming, the samples were stored in desiccator. The reason is to prevent oxidation of the surface exposed to cavitation, which can negatively influence the losses during the cavitation attack.

The total test duration of each sample was 165 min, divided into 12 periods (one for 5 and 10 min and 10 for 15 min). At the end of each test period, loss of material by cavitation erosion was determined by weighing. The assessment of cavitation erosion resistance was done by determining the average erosion depth, MDE and erosion rate curves, MDER, with the duration of attack.

Also, after completion of the cavitation attack tests (165 min), the eroded surfaces were subjected to roughness measurements and metallographic examinations.

Cavitation curves

Cavitation tests were run on sets of three samples for each heat treatment cycle, measuring the cumulative mean mass losses and based on them, the values of the mean erosion penetration depth, cumulated, MDE and speed penetration of erosion, MDER [2]:

$$MDE_i = \sum_{i=1}^{12} \Delta MDE_i = \frac{4 \cdot M_i}{\rho \cdot \pi \cdot d_p^2} \quad (1)$$

$$MDER_i = \Delta MDE_i / \Delta t_i \quad (2)$$

where:

- i - represents the test period;
- Δm_i - is the mass of material lost through erosion recorded during i, in grams;
- ρ - density of the cast iron, in g/mm^3 ;
- Δt_i - the duration of the cavitation corresponding to periods i (5, 10 or 15 min);

d_p - sample area diameter, cavitation attack ($d_p = 15.8 \text{ mm}$);

ΔMDE_i - the average depth of erosion penetration depth, achieved by cavitation during the period Δt_i .

In figure 2 and figure 3 are presented the evolutions in time of these two parameters characterizing the behavior of the iron investigated in the cavitation erosion.

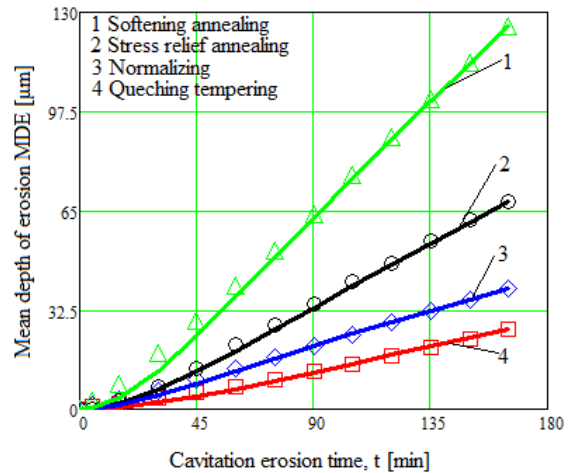


Fig. 2. Variation of the mean depth of erosion penetration with the duration of the cavitation attack

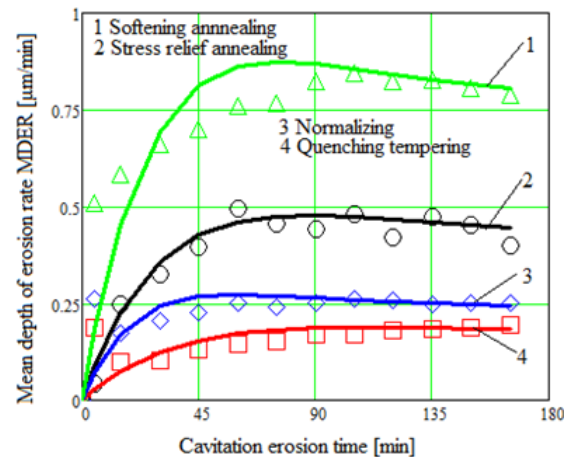


Fig. 3 The variation of the average depth of erosion penetration velocity with the duration of the cavitation attack

On the basis of these tests, there can be noticed significant differences in behavior of the same material depending on the microstructure obtained from the applied thermal treatments.

Thus, the most favorable values for MDEs and MDERs offer thermal treatment quenching + tempering, and the most unfavorable, thermal treatment for softening annealing.

Sufficiently good values are obtained after annealing for normalization, which can be applied either as a preliminary heat treatment or as a final heat treatment. By applying the normalization, a better resistance to vibration cavitation attacks is achieved as early as 45 min, when the MDER erosion rate (or the MDE (t) mass gradient slope decreases towards the stabilization value (about $0.245 \mu\text{m} / \text{min}$) in contrast to the annealing state for soaking at which the erosion penetration rate, after about 90 minutes, begins to fall to a stabilization value ($0.804 \mu\text{m} / \text{min}$).

At the same time, as compared to the thermal treatment of softening annealing, normalization provides a resistance increase of about 3.42 times the maximum value of the cumulative average depth of erosion (MDE curve (t)) and about 3.28 times the values to which stabilizes the speed parameter, MDER. These differences in cavitation behavior are justified by complete phase recrystallization caused

by heat treatment of normalization, with consequences on the finishing of the crystalline grains and the perlite matrix. Instead, thermal treatment for softening annealing is manifested by the decomposition of cementite traces in ferrite and graphite, as well as by a partial globalization of the perlite, both phenomena being accompanied by a decrease in hardness. The lower dispersion of the experimental values obtained for the erosion rate at the quenched and tempered samples is caused by the homogeneity of the microstructure and the improvement of the mechanical properties by applying this thermal treatment.

All this leads to a reduction of the average erosion depth of about 4.8 times and its speed of about 4.2 times, compared to the softening annealing, about 1.9 times and its speed of approx. 1.8 times compared to the structural state obtained for stress relief annealing.

Metallographic examinations

Electron microscopy investigations have shown that initiation of cavity tests of ferrite-perlite matrix samples initiates microgalvanic between graphite nodules and surrounding ferrite areas [16]. As a result of this phenomenon, the ferritic microstructure, anodic, will be able to dissolve the graphite nodule, which is cathodic. Therefore, the first surface attacked by the cavity consists of the ferrite-graphite interface. As the cavitation attack increases, a more pronounced separation of the graphite nodules from the surrounding ferrite takes place, a partial fragmentation of them and even the expulsion of some basic metal grains.

During this time, the pearlite, having a higher mechanical strength, will act as a protective skeleton against deformation of the surface. The end of the incubation period is reached after an intense deformation of the ferrite in the area of the limbs, when this soft phase will be the location of the priming of the cracks, and the areas of the material with pearlite microstructure will break through fatigue [2, 16]. The areas of material remaining after graphite expulsion have the form of pinholes or microcracks with high stress concentrators favoring the development of radial microfishes (fig 4).

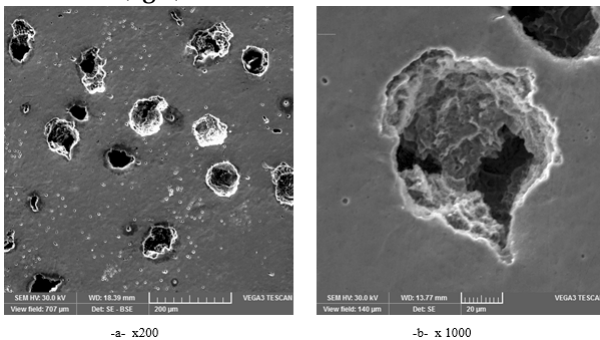


Fig. 4 SEM image (secondary electrons) of stress relief annealed cast iron, cavitated 15 min

Cavitation bubble implants with microjet jets justify the instantaneous production of strong local heating and high pressure. Such a pressure causes erosion to be triggered, and the total energy generated is transferred to the solid material, which can be absorbed or dissipated by it, as well as reflected as shock waves in the liquid. The absorption of impact energy by the solid material is manifested by the occurrence of elastic deformations, plastic deformations or ruptures [2, 13, 15].

In the case of ductile materials, cavitationally required, local plastic deformations were observed in the form of corrugations similar to the boundaries between grains and sliding strips [9, 12]. In defective areas, microforms with a

diameter of approx. 3 µm and representing the origin of some stress concentrations. Over time, these pinches suffer the phenomenon of coalescence, giving rise to tired microfishes.

The further increase of cavitation testing time causes an increase in the number of pinches and an increase in their coalescence with the formation of deep craters. The fatigue break mechanism becomes important and the wear particles will be removed as a result of the joining and growth of the microfishes.

Simultaneously with the degradation of the ferrite by cavitation, at the bottom of the holes caused by the graphite separation, one can observe the presence of a microtunnel. Its formation is probably a consequence of degradation of the material through microjet jets (fig. 5).

If the samples subjected to thermal treatment for stress relief annealing and softening annealing, the ferrite surrounding the graphite is strongly deformed [3, 16] by the application of thermal or normalization or quenching + tempering, an increase in hardness and mechanical strength, so that the deformation of the surface is lower [8].

Although the number of microforms formed by plastic deformation is significantly lower in hardened samples by thermal treatment, the developed microfishes suffer the phenomenon of coalescence, leading to the emergence of deep craters or microtunes (fig. 5b).

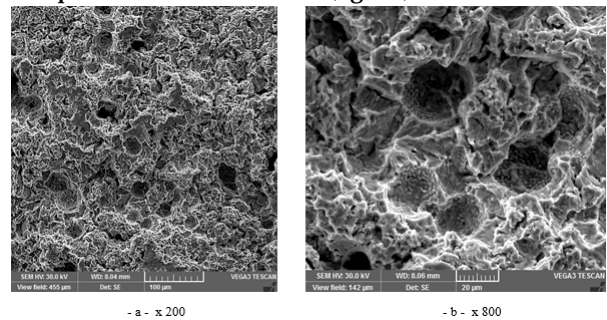


Fig. 5 The SEM image of the normalized samples area after 165 min of vibration cavitation erosion; a - pinch of material; b - microscale coalescence and formation of a microtunnel

Roughness measurements - correlation with cavitation resistance

Comparative analysis of the degree of damage to the surface following cavitation tests proves once again the beneficial effect of the thermal normalization treatments and especially of quenching tempering to the cavitation behavior of the studied iron. Even if after the removal of the graphite, which is a non-metallic inclusion, the respective portions of the surface of the material become more rough, in (fig. 6) it can be seen that the basic metal mass preserves more favorable values for the Ra and Rz parameters, if it has undergone the heat treatment of quenching tempering.

One of the parameters recommended by ASTM G32-2010 standards and which is used in the Cavitation Laboratory of U.P. Timisoara for assessing the surface resistance to cavitation erosion is the erosion rate, MDER. The opposite of this value, to which it tends to stabilize, MDERs - the final level, defines resistance to cavitation, R_{cv} table 1 shows the values of this rate, respectively cavitation resistance compared to those recorded for stress relief annealing, considered as reference treatment.

The data in this table clearly shows the substantial increase in resistance to vibration cavitation erosion, thermal annealing treatments for normalization and quenching followed by tempering. Instead, as expected annealing to soften, the surface resistance to impact with microjet jets induced by cavitation bubble implants

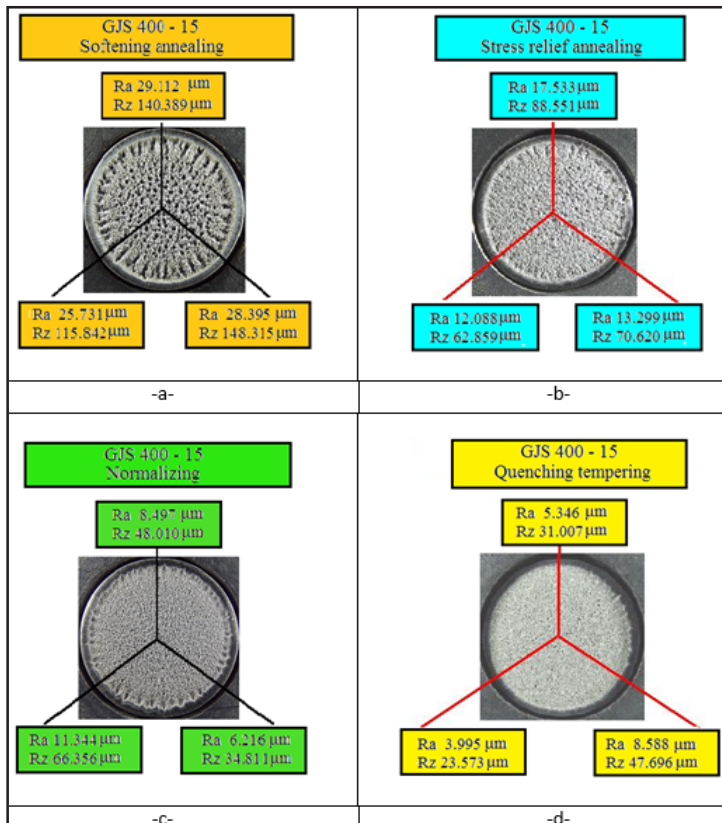


Fig. 6 Ra and Rz roughness values in three directions of measurement for the four structural states: a- softening annealing; b - stress relief annealing; c- normalizing; d- quenching tempering

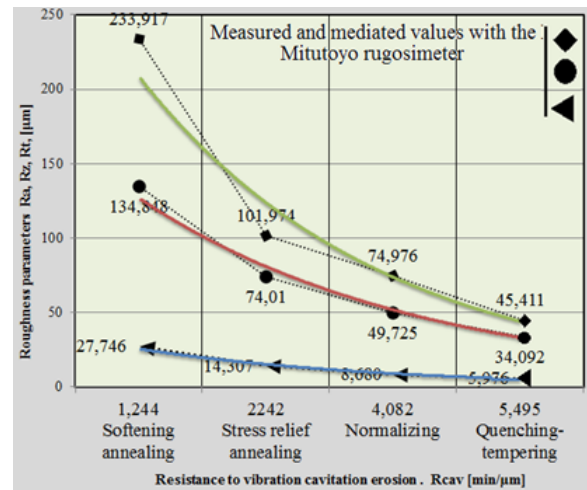


Fig. 7 Correlation between cavitation resistance and degraded surface roughness parameters

The treatment state of the sample	Resistance parameter to cavitation erosion		Resistance to stress relief annealing
	MDER _s [[μm/min]	R _{cav} [[min/μm]	
Softening annealing	0.804	1.244	Decrease with 80.23 %
Stress relief annealing	0.446	2.242	-
Normalizing	0.245	4.082	Increase with 82.07 %
Quenching tempering	0.182	5.495	Increase with 145.09 %

Table 1
THE RATE OF EROSION STABILIZATION MDERs AND CAVITATION RESISTANCE R_{cav}.

decreases. Figure 7 shows the variation of the three roughness parameters (Ra, Rz, Rt) with the surface vibration cavitation resistance ($R_{cav} = 1 / MDER_s$), depending on the thermal treatment applied. It can be noticed that, irrespective of the roughness parameter, the cavitation resistance is strongly influenced by the nature of the thermal volume treatment, the variance being an exponential one. This mode of variation is determined by the mechanical characteristics obtained as a result of the structural changes induced by the thermal treatment applied.

Hardness tests - correlation with surface roughness and cavitation resistance

Since hardness is the mechanical property most sensitive to structural changes in a metallic material, the samples in the four thermal treatment states have undergone such examinations. Generating these samples, eight Vickers hardness measurements were performed with a load of 5 daN/mm². The results obtained are centralized in (table 2), and on the basis of the average

No.	Stress relief annealing	Softening annealing	Normalizing	Quenching + tempering
1	209.5	171.5	317	471
2	204	174.5	342.5	441
3	207.5	171	332.5	483.5
4	205.5	174.5	340.5	463
5	215.5	187	339.5	480
6	226	179	349	450.5
7	219.5	193.5	362	448.5
8	214.5	178.5	374	460
Average value	212.8	178.7	344.6	462.2

Table 2
HARDNESS VICKERS HV5, NODULAR CAST IRON GJS-400-15

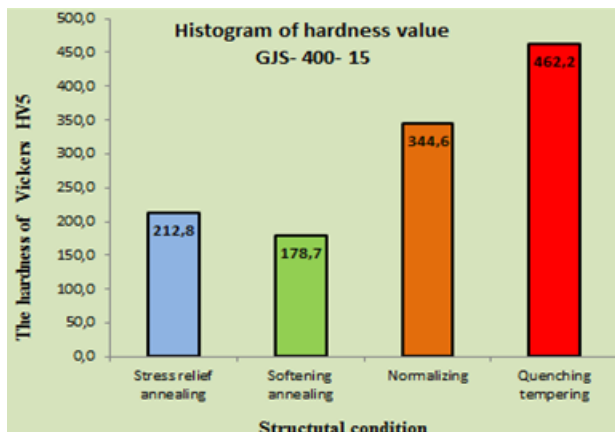


Fig. 8 Histogram of hardness values, GJS-400-15

values the histogram shown in (fig. 8) was constructed. The data presented demonstrate that there is a full concordance between the hardness and the opposite material resistance to degradation by cavitation erosion. The lowest hardness values are specific to the thermal treatment for softening annealing (about 178 HV5) and correspond to the highest erosion rate (0.804 $\mu\text{m} / \text{min}.$) and the worst roughness ($R_z = 134.8 \mu\text{m}$). Instead, the thermal treatment for quenching-tempering provides a high hardness (about 462 HV5) which favors a decrease in the erosion rate (0.182 $\mu\text{m} / \text{min}.$) and implicit minimum roughness values ($R_z = 34.09 \mu\text{m}$). It is noted that the parameter R_z was used because, according to the determination mode, it is similar to the cavitation MDE parameter at 165 minutes of testing.

The relationship between the hardness of the applied thermal treatments, the R_z roughness of the cavitationally tested surfaces for 165 min and the sizes that characterize cavitation behavior (MDERs, R_{cav}) is shown in (fig. 9). The higher the hardness, the lesser the roughness of the cavitationally attacked surface, and the cavitation behavior is better.

Conclusions

Cavitation degradation of ferrite-perlite nodules is triggered on the interface between ferrite and nodular graphite and is determined by microgalvanic activity and mechanical factors.

The topography of cavitationally tested surfaces demonstrates that the initiation of the cavitation phenomenon takes place on the ferrite-graphite interface and that with the increase of the duration of the attack a partial fragmentation and expulsion of the graphite nodules occurs

Compared to the softening annealing, the thermal normalization treatment provides an increase in the resistance of about 3.42 times the maximum value of the cumulative average depth of erosion (MDE (t) curve), respectively about 3.28 times the values to which stabilizes the speed parameter, MDER.

The increase in the proportion of perlite in the microstructure following the application of normalization justifies the improvement of cavitation resistance since this structural constituent, having higher mechanical strength characteristics, will resist deformation of the surface.

Applying the thermal quenching - tempering method causes a reduction of the average erosion depth of about 1.9 times and its speed of approx. 1.8 times compared to the structural state obtained by stress relief annealing.

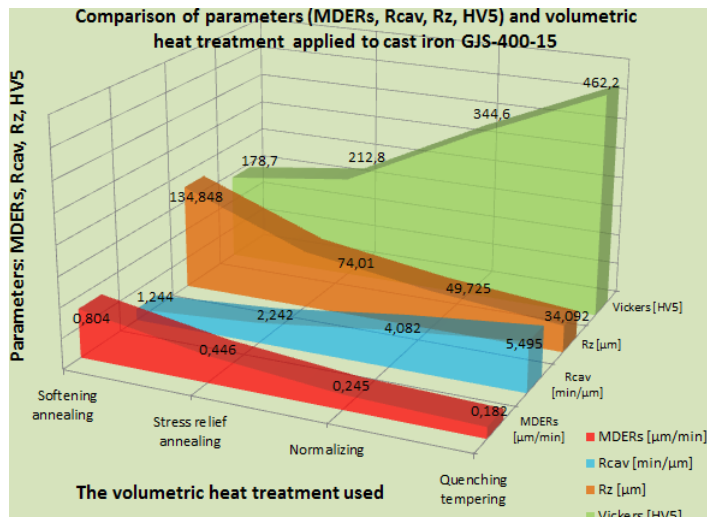


Fig. 9 Correlation between hardness, roughness and cavitation parameters of nodular cast iron GJS-400-15

The more or less spherical shape of the graphite along with the martensite matrix justifies the improvement of resistance to cavitation erosion.

The average roughness of the surface, R_a , tested at cavitation decreases from 14.307 μm (the stress relief annealing state) to 5.976 μm (the quenching-tempering state); the R_z roughness decreases from 74.01 μm (the stress relief annealing state) to 34.092 μm (the quenching-tempering state); the R_t roughness decreases from 101.974 μm (the stress relief annealing state) to 45.411 μm (the quenching-tempering state).

The comparison of the MDE cavitation resistance parameter (165 min) and the roughness parameter R_z shows that R_z is a good indicator of cavitation resistance and which, in the future, can be considered for the evaluation of this property.

Hardness measurements show a good concordance with cavitation resistance and roughness parameters at the end of the 165 min test period

References

- SHAMANIAN, M. MOUSAVI ABARGHOUE, S. M. R., MOUSAVI POUR, S. R., Effects of surface alloying on microstructure and wear behavior of ductile iron, *Materials & Design*, Vol. 31, No. 6, 2011, pp. 2760-2766
- BORDEASU I., Eroziunea cavitationala a materialelor, Editura Politehnica, Timisoara, 2006
- BENA, T. MITELEA, I., BORDEASU, I., CRACIUNESCU, C., The effect of the softening annealing and of normalizing on the cavitation erosion resistance of nodular cast iron FGN 400-15, *Metal 2016, International Conference on Metallurgy and Materials*, 2016, pp. 653-658, ISBN 978-80-87294-67-3
- ABBOUD, J. H., Microstructure and erosion characteristic of nodular cast iron surface modified by tungsten inert gas, *Materials & Design*, Vol. 35, 2012, pp. 677-684
- PODGORNIK, B., VIZINTIN, J., THORBJORNSSON, I., JOHANNESSON, B., THORGRIMSSON, J. T., MARTINEZ CELIS, M., VALLE, N., Improvement of ductile iron wear resistance through local surface reinforcement, *Wear*, Vol. 274-275, 2012, pp. 267-273
- FERNANDEZ-VICENTE, A., PELLIZZARI, M., ARIAS, J. L., Feasibility of laser surface treatment of pearlitic and bainitic ductile irons for hot rolls, *Journal of Materials Processing Technology*, Vol. 212, No. 5, 2012, pp. 989-1002
- ALABEEDI, K. F., ABBOUD, J.H., BENYOUNIS, K. Y., Microstructure and erosion resistance enhancement of nodular cast iron by laser melting, *Wear*, Vol. 266, No. 9-10, 2009, pp. 925-933
- BENA, T., MITELEA, I., BORDEASU I., UTU. I.D., CRACIUNESCU, C., The quenching - tempering heat treatment and cavitation erosion resistance of nodular cast iron with ferrite - pearlite microstructure,

Metal 2017, International Conference on Metallurgy and Materials, 2017, pp.118 - 123, ISBN 978-80-87294-73-4

9. HEYDARZADEH SOHI, M., EBRAHIMI, M., GHASEMI, H. M., SHAHRIPOUR, A., Microstructural study of surface melted and chromium surface alloyed ductile iron, Applied Surface Science, Vol. 258, No. 19, 2012, pp. 7348- 7353

10. BORDEASU, I., MICU, L. M., MITELEA, I., UTU, I. D., PIRVULESCU, L. D., SIRBU, NICUSOR, A. N., Cavitation Erosion of HVOF Metal-ceramic Composite Coatings Deposited onto Duplex Stainless Steel Substrate, Mat. Plast., **53**, no. 4, 2016, p. 781

11. MITELEA, I., BORDEASU, I., UTU, I. D., KARANCSI, O., Improvement of the Cavitation Erosion Resistance of Titanium Alloys Deposited by Plasma Spraying and Remelted by Laser, Mat. Plast., **53**, no. 1, 2016, p. 29

12. BENYOUNIS, K. Y., FAKRON, O. M. A., ABOUD, J. H., OLABI, A. G., HASHMI, M. J. S., Surface melting of nodular cast iron by Nd-YAG laser and TIG, Journal of Materials Processing Technology, Vol. 170, No. 1-2, 2005, pp. 127-132

13. ZENKER, R., BUCHWALDER, A., RUTHRICH, K., GRIESBACH, W., NAGEL, K., First results of a new duplex surface treatment for cast

iron: Electron beam remelting and plasma nitriding, Surface and Coatings Technology, Vol. 236, 2013, pp. 58-62

14. YAN, H., WANG, A., XIONG, Z., XU, K., HUANG, Z., Microstructure and wear resistance of composite layers on a ductile iron with multcarbide by laser surface alloying, Applied Surface Science, Vol. 256, No. 3, 2010, pp. 7001-7009

15. MITELEA, I., BORDEASU, I., MICU, L.M., CRACIUNESCU, C.M., Microstructure and cavitation erosion resistance of the X2CrNiMoN22-5-3 Duplex stainless steels subjected to laser nitriding, Rev. Chim. (Bucharest), **68**, no. 12, 2017, p. 2992

16. MITELEA, I., BORDEASU, I., PELLE, M., CARCIUNESCU, M.C, Ultrasonic cavitation erosion of nodular cast iron with ferrite-pearlite microstructure, Ultrasonic Sonochemistry, Vol. 23, 2015, pp. 385-390

17.*** Standard test method for cavitation erosion using vibratory apparatus ASTM G32-2010

18. BORDEASU, I., MITELEA, I., LAZAR, I., MICU, L.M., KARANCSI, O., Cavitation Erosion Behaviour of Cooper Base Layers Deposited by HVOF Thermal Spraying, Rev. Chim. (Bucharest), **68**, no. 12, 2017, p. 2914

Manuscript received: 11.10.2017